Improvements in the analysis of diffraction phenomena by means of digital images

A. Ramil, A. J. López, and F. Vincitorio

Additional information on Am. J. Phys.

Improvements in the analysis of diffraction phenomena by means of digital images

A. Ramil[a)] and A. J. López
Deparatmento de Enxeñaría Industrial II, Universidade da Coruña, E15403 Ferrol, A Coruña, Spain

F. Vincitorio
Facultad Regional Paraná, Universidad Tecnológica Nacional, Almafuerte 1033, Paraná, Entre Ríos, Argentina

We introduce a simple methodology employing digital photography and image processing techniques to do a quantitative study of diffraction. To enhance the range of intensities recorded by a CCD camera without saturation, digital images of the diffraction patterns taken at different exposure times are combined pixel by pixel, and the measured values of the light intensity are fitted to theoretical curves. Diffraction by a single slit, a double slit, and a circular hole were analyzed to obtain quantitative results and demonstrate that the methodology is suitable for student laboratories. © *2007 American Association of Physics Teachers.*
[DOI: 10.1119/1.2772288]

I. INTRODUCTION

The use of digital image techniques to demonstrate basic concepts in physics was initiated in the 1990s[1–6] and has increased recently due, in great part, to the low cost of digital cameras and the development of digital image processing software.[7–19]

One of the limitations of digital cameras, especially in the field of optics, is the possibility of saturation of the pixel signals. This problem has been alleviated in some cases by using filters to reduce the intensity of the light reaching the CCD.[4–7] In diffraction there are great differences between the intense central spot and secondary maxima, and thus the use of filters can lead to a loss of information about the less intense areas and make it difficult to do a quantitative analysis.

The methodology proposed in this paper for the analysis of diffraction is based on the combination, pixel by pixel, of images with exposure times that are adequate for measuring the different intensity levels in the pattern. Most digital cameras record images in a JPEG file, which can be read by photoediting software, which works with the 24 bits in RGB format or 8 bits in grayscale. By combining the different images it is possible to enhance the range of intensities over the 8 bits and thus obtain the intensity profile of the complete diffraction pattern.

The aim of this paper is to improve the quality of student experiments on diffraction by using a simple methodology that exploits the advantages of digital techniques to record diffraction patterns and to manipulate image files. Simple calibrations let students convert pixel numbers to position to high accuracy and thereby perform a quantitative analysis of the intensity profiles by fitting them to theoretical curves.

II. EXPERIMENTAL SETUP

A schematic of the experimental setup to obtain images of the diffraction patterns is shown in Fig. 1. We used a Uniphase 0.5 mW, $\lambda=632.8$ nm He–Ne laser with random polarization and transverse mode TEM_{00}. To increase the laser divergence and ensure a uniform illumination of the slit, a divergent lens ($f=-100$ mm) was employed. Images of the diffraction patterns were obtained by using a Nikon D100 digital camera with exposure times ranging from 30 to 1/4000 s and an objective Nikon micro 60/2.8. The CCD of the camera consists of 6.1×10^6 pixels and presents an active area of 23.7×15.6 mm^2.

A glass diffuser was situated in the optical path and the camera was focused on it. To perform a spatial analysis of the diffraction pattern, the diffuser was removed and replaced by a ruler to obtain the calibration factor that transforms pixels (in the focal plane of the camera) into distances (in the plane of the diffuser).

To avoid vibrations the camera was connected to a computer via the USB port, and pictures were taken with a keyboard command without touching the camera. The lens aperture and focusing were manually operated, and the rest of the process was controlled via Nikon capture software. The exposure time can be set automatically or manually for a given aperture. The computer was also used for visualizing, storing, and analyzing the images.

III. EXPERIMENTAL PROCEDURE

To develop a methodology for image capturing, the non-uniformity of the intensity distribution in diffraction patterns must be taken into account. Typically a bright central maximum accompanied by secondary maxima that are several orders of magnitude less intense can be observed. This dramatic intensity difference causes problems because for a given aperture of the camera and exposure time, there will be areas in the digital image where the pixel signals reach the saturation level while other areas remain hardly visible.

The proposed method to overcome this problem without losses of information consists in recording images at different exposure times (see Fig. 2). Pictures corresponding to the lower exposure give information about the intense central
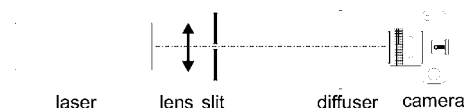

Fig. 1. Experimental setup to obtain digital images of the diffraction patterns.
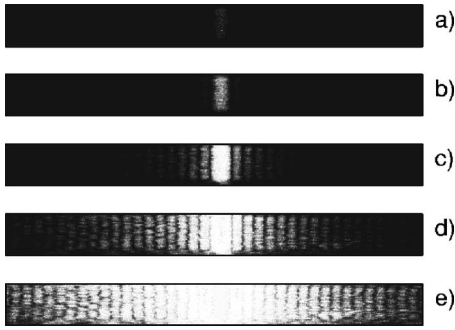
Fig. 2. Images of single slit diffraction patterns taken at increasing exposure times: (a) 1/4000, (b) 1/250, (c) 1/15, (d) 1, and (e) 15 s.

Fig. 4. Plot of the resulting intensity profile of the single slit diffraction pattern. The pixel number has been converted to millimeters.

area. By increasing the exposure time information of the secondary maxima, can be obtained, although saturation might be reached in the central area. These pictures can be combined pixel by pixel to acquire a complete image of the diffraction pattern.

First, pictures must be converted to 8 bit grayscale, that is, 256 levels. Then, the combination of the series of images (I_k; $k=0,\dots,n-1$) with increasing exposure times t_k in a nonsaturated new image I_0 can be performed as follows:

1. The first picture is considered as the initial image I_0. This image should not be saturated and has the shortest exposure time, t_0.
2. In the image I_k, nonsaturated pixels (gray level lower than 90% of the maximum value, 255) are located.
3. The nonsaturated pixels, NS, are used to replace the values in I_0. To take into account the different exposure times in image I_0 and image I_k, a correction factor t_0/t_k was introduced so that $I_0(NS)=I_k(NS)t_0/t_k$.
4. Steps 2 and 3 are repeated for k from 1 to $n-1$.

The resultant image contains the intensity of each pixel corresponding to the picture with higher exposure without saturation.

To facilitate the task, a software package was written using MATLAB.[21] In brief, the software reads the image files, shows the image on the screen, plots the intensity profiles at the center of the image, and shows the location of the saturated pixels (a nonsaturated image for each case is necessary). The user has only to select the image files to be combined. Time exposure, F number, and other characteristics, are obtained directly from the JPEG image files.

IV. ANALYSIS OF DIFFRACTION PATTERNS

Measurements for single slits, double slits, and circular holes were recorded and the intensity profiles were analyzed by fitting experimental values to theoretical curves for Frauhoffer approximation.[20]

A. Single slit

A single-slit diffraction pattern at exposure times of 1/4000; 1/250, 1/15, 1, and 15 s are shown in Fig. 2. The visible areas of the pattern increase with exposure time and saturation becomes appreciable.

A digital image consists of an array of pixel intensities distributed in rows and columns. In Fig. 3 the intensity profiles calculated as the average column values in the digital images are plotted. The saturation threshold corresponds to 90% of the maximum value, 255. In Fig. 3(a), corresponding to the lowest exposure time, all the pixels are less than the saturation level; increasing the exposure to 1/250 s causes only the central maximum to be visible but some pixels are saturated [Fig. 3(b)]; for 1/15 s the first three secondary fringes of the diffraction pattern can be observed but the central maximum is clearly saturated [see Fig. 3(c)].

The exposure times that have been selected give a intensity ratio of around 16 between two consecutive images. Therefore, each additional image increases the intensity range from the previous one by 4 bits. In Fig. 4 the resulting intensity profile, converted from pixel number to position, is shown. Note that the intensity range covers more than 4 orders of magnitude, which corresponds to more than 15 bits.
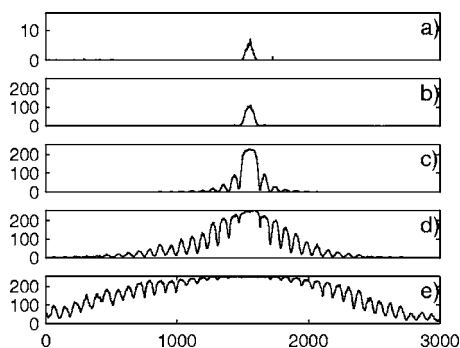

Fig. 3. Intensity profiles obtained as the average column values of the images at exposure times (a) 1/4000, (b) 1/250, (c) 1/15, (d) 1, and (e) 15 s.
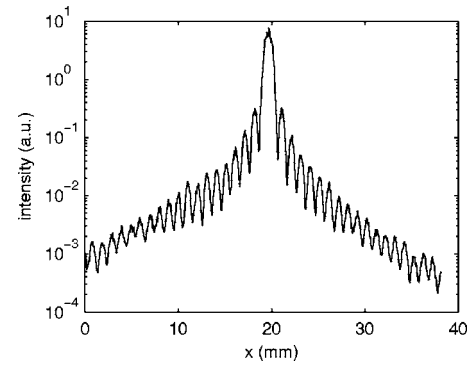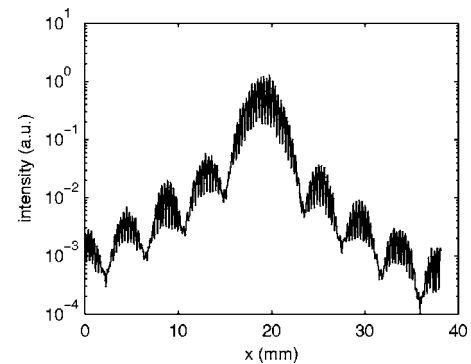

Fig. 5. Plot of the resulting intensity profile of the double slit diffraction pattern.

Table I. Values of the slit width b and results from the fit.

Supplier	Results from Fit		
b (μm)	b (μm)	σ_b (μm)	R^2
160	155.8	0.8	0.9861
80	85.7	0.4	0.9834
40	40.76	0.16	0.9901
20	20.48	0.09	0.9861

The values of the intensity were fitted to the Fraunhoffer equation for a slit width b:

$$I(\theta) = I(0)\frac{\sin^2 \beta}{\beta^2}, \tag{1}$$

where $\beta = kpb/2$, $k = 2\pi/\lambda$, $p = \sin \theta = (x-x_0)/\sqrt{(x-x_0)^2 + L^2}$, x is the position in the picture normal to the slit, x_0 is the center of the diffraction pattern, and L is the distance from the slit to the screen (diffuser). A nonlinear least squares fit of $I(x)$ using the known values of L and λ is used to estimate b and x_0 and their confidence bounds. The slit width uncertainty σ_b is obtained as one half of the interval for a 95% confidence level. The experimental values of b for different slits are summarized in Table I. These results confirm the quality of the method.

B. Double slit

By following the same procedure a complete diffraction pattern produced by a double slit arrangement was recorded; the intensity values are plotted in Fig. 5. The pattern consists of a set of narrow, equally spaced fringes superimposed on the single-slit diffraction intensity envelope.

The intensity corresponding to a double slit of width b and distance between centers a is given by

$$I(\theta) = I(0)\frac{\sin^2 \beta}{\beta^2} \cos^2 \alpha, \tag{2}$$

where $\alpha = kpa/2$. The interference term, $\cos^2\alpha$, multiplies the diffraction pattern of a single slit given by Eq. (1). Different values of a and b were tried, and the results are summarized in Table II. As before, the calculated values are in agreement with the value given by the manufacturer.

C. Circular hole

Due to the radial symmetry of the pattern, the procedure to obtain the intensity distribution must be slightly different.

Table II. Supplier and experimental values obtained for the double slit arrangement.

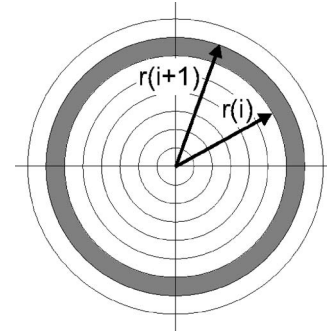| Supplier		Results from Fit				
a (μm)	b (μm)	a (μm)	σ_a (μm)	b (μm)	σ_b (μm)	R^2
500	40	508.2	0.3	38.0	0.4	0.9366
250	40	248.4	0.2	36.7	0.2	0.9757
125	40	128.4	0.2	43.0	0.2	0.9823
250	80	248.9	0.3	78.5	0.3	0.9909
500	80	502.0	0.9	71.2	1.0	0.8816

Fig. 6. Slices to calculate the intensity distribution for diffraction by a circular hole.

First, the coordinates of the geometric center of the image were calculated by fitting the first minimum to the equation for the circumference. Then, the pattern was cut into 100 circular slices (see Fig. 6). For a given radius, the intensity was calculated as the sum of the pixel intensities in the slice between $r(i)$ and $r(i+1)$. The resulting intensity values, plotted in Fig. 7, were fitted to the relation

$$I(\theta) = I(0)\left[\frac{J_1(kpw)}{kpw}\right]^2, \tag{3}$$

where $k = 2\pi/\lambda$, $p = \sin \theta = r/\sqrt{r^2 + L^2}$, $w = D/2$ is the radius of the hole, and $J_1(x)$ is the Bessel function of the first kind.

In this experiment the diameter of the hole was $D = 80$ μm. The experimental values of D, calculated at different distances L, are shown in Table III as "fit 1." The experimental values are far from the correct ones. This discrepancy can be attributed to the great difference between the intensity in the central maximum and the rest of the diffraction pattern, which leads to the points in the central maximum having a much higher weight in the fit than points outside the maximum.

The best results are obtained using the position of the minima of the diffraction pattern, x_n. These values were calculated by means of a cubic spline interpolation function for the intensity profile. The zeroes of the first derivative when the second derivative is positive give the position of the minima. By fitting these minima to the zeroes of $J_1(x)$ ($x = 3.831705970, 7.015586670, 10.17346814, \ldots$), the slope provides a new and more realistic estimate of the hole diameter, summarized in Table III as "fit 2."
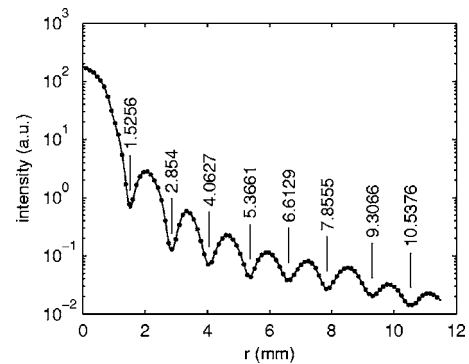

Fig. 7. Plot of the intensity profile of the circular hole diffraction pattern. The numbers inside the plot indicate the radius of the minima.

Table III. Experimental values of the hole diameter D at different distances L, obtained by fitting the intensity profile to the Fraunhoffer equation (fit 1), and by fitting the minima of the diffraction pattern to the zeroes of $J_1(x)$ (fit 2).

Distance L (cm)	Fit 1			Fit 2		
	D (μm)	σ_D (μm)	R^2	D (μm)	σ_D (μm)	R^2
50	72.8	0.8	0.9783	72.1	1.4	0.999998
25	68.3	0.6	0.9984	72.7	1.2	0.999919
15	68.2	0.5	0.9991	76	2	0.999292

V. SUMMARY

We have reported on a simple method based on the use of a digital photo camera and computer image processing to perform quantitative experiments in Fraunhoffer diffraction. This methodology lets us obtain reliable quantitative data, avoiding the use of filters, which diminish the intensity and cause the loss of information about the diffraction pattern.

By employing this methodology students can quickly and routinely record diffraction patterns. Simple calibrations allow them to convert pixel numbers to position to a high degree of accuracy. This technique can also be used for other photometric applications.

[a]Electronic mail: aramil@cdf.udc.es

[1] A. G. Podoleanu, S. R. Taplin, D. J. Webb, and D. A. Jackson, "Channelled spectrum display using a CCD array for student laboratory demonstrations," Eur. J. Phys. **15**, 266–271 (1994).

[2] K. H. Elliott and C. A. Mayhew, "The use of commercial CCD cameras as linear detectors in the physics undergraduate teaching laboratory," Eur. J. Phys. **19**, 107–117 (1998).

[3] M. P. Silverman and W. Strange, "The Newton two-knife experiment: Intricacies of wedge diffraction," Am. J. Phys. **64**, 773–787 (1996).

[4] G. R. Wein, "A video technique for the quantitative analysis of the poisson spot and other diffraction patterns," Am. J. Phys. **67**, 236–240 (1999).

[5] C. Lengacher, S. Macklin, D. Hite, and M. F. Masters, "Low cost CCD detectors for spectroscopy," Am. J. Phys. **66**, 1025–1028 (1998).

[6] C. de Izarra and O. Vallee, "On the use of linear CCD image sensors in optics experiments," Am. J. Phys. **73**, 986–990 (2005).

[7] O. Van Overschelde and M. Wautelet, "Self-difraction in a CCD camera," Eur. J. Phys. **26**, 15–17 (2005).

[8] S. Gil, H. D. Reisin, and E. E. Rodriguez, "Using a digital camera as a measuring device," Am. J. Phys. **74**, 768–775 (2006).

[9] N. A. Gross, M. Hersek, and A. Bansil, "Visualizing infrared phenomena with a webcam," Am. J. Phys. **73**, 986–990 (2005).

[10] P. Nakroshis, M. Amoroso, J. Legere, and C. Smith, "Measuring Boltzmann's constant using video microscopy of Brownian motion," Am. J. Phys. **71**, 568–573 (2003).

[11] J. Peatross and M. V. Pack, "Visual introduction to Gaussian beams using a single lens as an interferometer," Am. J. Phys. **69**, 1169–1172 (2001).

[12] L. Repetto, F. Pellistri, E. Piano, and C. Pontiggia, "Gabor's hologram in a modern perspective," Am. J. Phys. **72**, 964–967 (2004).

[13] M. Vannoni and G. Molesini, "Speckle interferometry experiments with a digital photocamera," Am. J. Phys. **72**, 906–909 (2004).

[14] R. Cross, "Measurements of the horizontal coefficient of restitution for a superball and a tennis ball," Am. J. Phys. **70**, 482–489 (2002).

[15] T. Greczylo and E. Debowska, "Using a digital video camera to examine coupled oscillations," Eur. J. Phys. **23**, 441–447 (2002).

[16] J. A. Monsoriu, M. H. Gimenez, J. Riera, and A. Vidaurre, "Measuring coupled oscillations using an automated video analysis technique based on image recognition," Eur. J. Phys. **26**, 1149–1155 (2005).

[17] M. E. Saleta, D. Tobia, and S. Gil, "Experimental study of Bernoulli's equation with losses," Am. J. Phys. **73**, 598–602 (2005).

[18] K. J. Silva and J. C. Mahendra, "Digital video microscopy in the Milikan oil-drop experiment," Am. J. Phys. **73**, 789–792 (2005).

[19] B. T. King and W. Tobin, "Charge-coupled device detection of two-beam interference with partially coherent light," Am. J. Phys. **62**, 133–137 (1994).

[20] Max Born and Emil Wolf, *Principles of Optics: Electromagnetic Theory of Propagation, Interference and Diffraction of Light*, 6th ed. (Pergamon, Oxford, 1980).

[21] See EPAPS Document No. E-AJPIAS-75-012710 for the software written for MATLAB and example images. This document can be retrieved through a direct link in the online article's HTML reference section or via the EPAPS homepage (http://www.aip.org/pubservs/epaps.html).